

# Design of a Miniaturized Flexible Patch Antenna with Shorting-Pin Integration for Enhanced Gain in RFID, ISM, and Wearable Biomedical Applications

Waqas Ali<sup>1</sup>, Nizam-Ud-Din<sup>2</sup>, Muhammad Zahid<sup>3\*</sup>

<sup>1</sup>Department of Electrical Engineering, HITEC University Taxila, Pakistan,

<sup>2</sup>Department of Biomedical Engineering, HITEC University Taxila, Pakistan

<sup>3</sup>Department of Telecommunication Engineering, University of Engineering and Technology Taxila, Pakistan,

\*Correspondence: [muhammad.zahid@uettaxila.edu.pk](mailto:muhammad.zahid@uettaxila.edu.pk)

**Citation** | Ali. W, Din. N. U, Zahid. M, "Design of a Miniaturized Flexible Patch Antenna with Shorting-Pin Integration for Enhanced Gain in RFID, ISM and Wearable Biomedical Applications", IJIST, Vol. 7 Issue. 4 pp 3112-3132, December 2025

**Received** | November 09, 2025 **Revised** | November 26, 2025 **Accepted** | December 06, 2025

**Published** | December 12, 2025

Antennas are integral parts of wireless communication because they can ensure that signals are transmitted and received effectively, encompassing a variety of frequencies, such as those used in IoT and overall RF systems. This paper introduces a miniaturized single-band antenna of  $9 \times 31.6 \times 0.254$  mm<sup>3</sup> with a specific design for wearable applications, which was made on flexible Rogers RT5880 substrate. Using the CST Microwave Studio 2024 microchip as the design and analysis tool, the proposed antenna consists of a rectangular slot-based radiating structure with a shorting pin and probe feed, which can achieve stable design performances both in the free-space and on-body situation services. Compliant with the wearable safety requirements and operating at a low level specific absorption rate (SAR) less than 1.6 W/kg at the resonant frequency. The antenna has good radiation performance, with a maximum efficiency of 82% and a maximum gain of 4.1 dBi, having a bidirectional radiation pattern in the elevation plane and an omnidirectional radiation pattern in the azimuth plane. The introduction of shorting-pin as a strategic method of reducing the length of resonance allows the approach of substantial reduction in the resonant length without compromising radiation characteristics. Simulation results also provide further confidence scales of stabilizing impedance performance and omnidirectional radiation pattern properties in the target 5.725-5.875 GHz ISM band, which demonstrates the expectation of shorting-pin strategies for the development of small-size, high biocompatibility, and flexible antennas for next-generation wearable, body-area network, and radio frequency identification (RFID) communication systems.

**Keywords:** RFID Antennas; ISM Band; Patch Antenna; IoT and IoE, Biomedical and Wearable Applications.



TOGETHER WE REACH THE GOAL



## Introduction:

The sudden increase in complex wireless applications has led to the speedy development of the radio frequency identification (RFID) technology largely because of its wide range of applications with regard to the functions that it performs, such as detecting, monitoring, tracking, and data collection. These capabilities make RFID a useful solution for a variety of different fields and include access control, electronic transportation payment systems, security infrastructures, livestock management, and healthcare operations[1].

RFID systems can be categorized into active and passive depending on the existence of a built-in power source, the former being used to identify, track, and localize objects, and in various types of IoT applications. These systems are operated over a wide range of frequency ranges, i.e., 125-134 kHz (low frequency), 13.56 MHz (high frequency), 869 MHz & 902-928 MHz (Ultra High Frequency), 2.45 GHz (2.4-2.483 GHz), 5.8 GHz (5.725-5.875 GHz) & 24 GHz (Microwave Frequencies). Lower frequency bands, with their longer waves, necessitate a much larger size for the tag itself as well as small read ranges, while super high frequency (SHF) bands allow for much faster speeds of tracking, up to 40 meters per second, supporting applications such as vehicle monitoring at toll booths and goods management [2]. Here, the frequency band of 5.7 GHz is chosen as the frequency range of the design and analysis of the RFID system. This choice is driven by the fact that it is allocated in the well-known ISM (Industrial, Scientific and Medical) frequency band, where unlicensed operation is possible, and that wide compatibility with existing wireless and RFID technologies can be expected. Operating at 5.7 GHz also allows for the construction of a small antenna while still ensuring sufficient bandwidth and gain to fit into applications that have space or other physical constraints, such as handheld readers and dense storage environments. Furthermore, many modern systems of the radio-frequency identification (RFID) and the Internet of Things (IoT) work in this band, and this ensures that the proposed design is practical and in step with present-day requirements in the industrial and research world.

Miniaturization of the antennas for the readers is a key requirement as it facilitates integration with a portable reader such as a handheld reader, deployment of the reader in a space-constrained environment such as a dense warehouse environment, material utilization, and system cost. In order to meet the increasing demand for space-saving ground-based antenna designs, various miniaturization techniques of the antenna have been proposed in the literature. One common strategy for miniaturization involves the use of folded geometries, where the alteration of the shapes of the radiating elements is effectively used to minimize the physical footprint of an antenna. Another approach that is widely used is the introduction of shorting elements; the introduction of shorting patches will allow capacitive loading between the radiating patch element and the ground plane, lowering the resonant frequency and thus reducing the antenna size. Artificial Magnetic Conductors (AMCs) have also been used. Some of the research on using an AMC layer under the antenna has shown that the profile of the antenna can be even further reduced. Finally, sidewall space utilization is achieved by folding the feeding network / radiating structures onto vertical spaces, thereby minimizing the overall aperture of the antenna[3][4][5][6][7][8][9].

As a result, the trend in more recent research on the role of radio frequency identification (RFID) is to concentrate on the microwave frequencies because of the benefits of a smaller tag size, whilst still offering greater read distance and data rate[10]. One popular miniaturization technique is to increase the electrical length of the antenna to further increase the distance for current flowing and yield more compact tag designs with improved performance. Over the past two decades, many techniques have been investigated that enable the realization of miniaturized chips with an antenna, among others, including the realization of a conductive layer between patch elements, which increases capacitive reactance and therefore further reduces the size of the antenna[11].

Another miniaturization method is placing a non-resonating ring below a dipolar patch antenna, proposed a different method that uses an edge-shortened slot microstrip antenna comprised of a rectangular radiating element, the shorting wall, and a pair of shorting strips as an effective way to reduce the antenna size while preserving the performance[12].

In addition, a planar inverted-F antenna (PIFA) has been proposed, which is a dual-layer antenna fed by the proximity coupling model, specifically designed for the UHF frequency[13].

Some other methods of miniaturization include folded slots short monopoles with a folded slot inside a rectangular patch, and the folded slots on a half ring of a rectangular patch. Edge-shortened slots with shortening walls and strips were also used. In addition, meandered coplanar waveguide feed line and metamaterial-inspired hexagonal split ring resonator (SRR) radiating structures were used. Another design, a planar complementary dipole antenna based on a combined aperture-dipole structure, was offered.

Aslam et al. in 2016, 2017, and 2019 investigated additional miniaturization techniques, such as comb-like etchings on the patch and modified H-shaped slots to further reduce the size of the antenna. For dual-band antennas, several approaches to size reduction have been studied, like U-slots and complementary split ring resonators (CSRR), and the utilization of two identical slots has also been investigated to obtain small-size dual-band antennas. A popular route to be able to further miniaturize is the inclusion of fractal geometries, such as the Koch and Sierpinski fractals, which have been applied successfully in designs of the Radiotelephones (RFD) antennas for the enlargement of the electrical length with a compact footprint[14].

In recent years, miniaturized antenna design that can be used with high efficiency at the targeted frequencies has become a more important task. One effective way to do this is through finding methods of increasing the electrical length of the antenna by increasing the path of current, and this can be achieved with fractal structures without physically doing so. Fractals, with their inherent qualities of self-similarity and recurring features at multiple scales of size, are of specific interest for antenna miniaturization because they allow for longer current paths in small geometries. Inspired by fractal principles, the structure of Spidron, the structure in which every single element is a triangle, provides a way to iterate the current path and contributes to the size reduction. Although several antennas have been developed using Spidron fractal geometry, many of them have shown no particular interest in miniaturization[15][16][17][18][19].

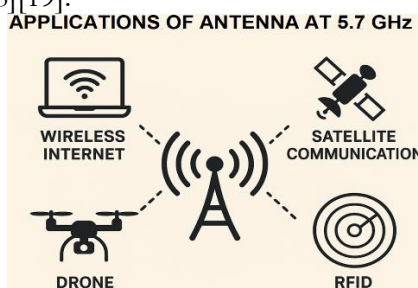


**Figure 1.** Applications of the Proposed Antenna

Figure 1 shows the wide variety of applications of antennas using 5.7 GHz and demonstrates their important role in contemporary wireless communications systems. In the center, there is a tower of radio antennas that represents the heart transmitter or receiver of signal waves. Surrounding it are 4 classes of important applications linked by dotted lines: Wireless Internet, which refers to Wi-Fi and other similar technologies; Satellite Communication, which denotes data transmission to and from a satellite; Drone operations, which involves remote control and data links for unmanned flying vehicles; and RFID (Radio Frequency Identification) which is used widely for tracking and identification purposes for

logistics and inventory management. This picture stresses the versatility and importance of antennas at the frequency band of 5.7 GHz for different cutting-edge technological fields.

Wearable and flexible electronics have spurred a great deal of interest in both the industrial and the academic world, thanks to their versatility and broad range of possible applications, such as personal devices, the Internet of Things (IoT), sports monitoring, military systems, radio frequency identification (RFID), medical body area networks (MBANs), etc. In the past years, microstrip patch antennas have received great attention for wearable applications because of their lightweight structure, simple design, compact size, easy fabrication, frequency tunability, and compatibility with planar circuits. However, traditional antenna structures have an overall rigid structure and rigid design, which cannot meet the requirements of wearable spaces where flexibility and comfort of the wearer are most important. The effectiveness of the wearable antenna depends on various critical factors that involve passive operation, small size, low weight, efficient costing, and maintenance-free functions, which have a direct effect on the wearability and easy movement of the user. To solve such problems, numerous flexible substrate materials such as textile, denim, polyfoam, polyethylene terephthalate (PET), glass, conductive fabric polymer, felt, polyimide, and cotton fabrics have been examined for flexible antenna material design to improve the flexibility and conformability of the antenna. Many recent studies have used these substrates for working at conventional frequencies, especially 2.45 GHz. Nevertheless, antenna designs for this frequency band may experience limitations in data rates that can be achieved and sometimes even higher design complexity[20][21].

In recent years, the need for sophisticated systems using microwaves and millimeter wave frequencies has grown as a result of the increasing difficulty of communications in terms of antenna size, bandwidth, and gain. Consequently, antennas are now key components for a wide range of applications in satellite communications, which will operate at different frequency bands. Researchers are still trying to improve bandwidth and gain to satisfy these requirements. With the fast development of technology, wireless communication has developed to a very advanced level, and both developed and developing countries are relying on the wireless communication systems extensively [22][23][24][25]. The intertwining of high-performance materials along with fresh design approaches like metamaterials and metasurfaces has shown great potential to promote higher performance of antennas while minimizing their size. These approaches are aimed at optimizing important parameters, such as bandwidth, gain, isolation, and general efficiency, to address the complex requirements of IoT applications that are enabled by the adoption of an RFID approach[26][27]. At the heart of robust communication in IoT systems is the antenna - it is the key interface of data transfer. However, traditional single-band antennas cannot keep up with the requirements of modern IoT systems. Although multifrequency antennas have been designed to be in multiple frequency bands, their design is limited by the amount of space available in small devices and the complexity of nearby electronics. The explosion in popularity of the Internet of Things (IoT) is fueling the need for compact and energy-saving components to enable the increasingly pervasive wireless communication. This work investigates endogenous integration of hybrid metamaterials for the power efficiency and miniaturization of microwave amplifiers. In the case of other concepts, like the storage environment of RFID systems, it is the interaction between the tag and the reader antenna that is a critical factor. A popular practical solution is to have several CP reader antennas in order to get a larger reading range and effectively handle large quantities of items. Nevertheless, designing a CP antenna that can simultaneously provide wide beamwidth, high performance, and low cost is still a huge challenge[28][29][30].

Compact wideband directional antennas are becoming a hot demand in applications such as UWB communication for wearable devices, UWB radar and imaging systems, wireless body area networks, and retransmission-based chipless RFID systems. Various miniaturization

methods have been proposed in the literature for-size reduction of tapered slot antenna (TSA). These methods can be broadly grouped as follows: (1) the introduction of slots of different shapes along the edges of the ground conductor, (2) introducing corrugations at the sides of the ground conductor, and (3) changing the tapered slot geometry. The other common miniaturization method is the use of corrugations on the sides of the ground conductor of tapered slot antennas (TSAs). Corrugations consist of a periodic arrangement of uniform or nonuniform slits, which can be rectangular, triangular, trapezoidal, or arbitrary. Beyond the benefit of reducing size, the corrugations can also be used to improve gain and provide better distribution. For example, a compact coplanar waveguide-fed TSA with three pairs of trapezoidal slots was proposed to operate over a frequency band from 3 GHz to 11.4 GHz. The changes in the number of slot pairs, including both the reduction of size and enhancement of gain, are still areas of investigation. Additionally, the miniaturization capability of rectangular, cosine, and sawtooth (triangular) corrugations embedded in TSAs using multi-section binomial transformers has been compared for UWB applications[31][32][33][8][34].

Recently, meta-surface-based antennas and their arrays that provide high gain and unique electromagnetic characteristics missing in natural materials have received much attention in research. For example, in a meta surface-based antenna array in mm-wave MIMO application, an enhanced gain of 10.27 dBi was achieved with a relatively narrow bandwidth of 1.95 GHz. Another work suggested a planar and vertically polarized (VP) end-fire antenna using the trapped wave technique. By combining a four-element series-fed magnetic dipole array inside a dual-layer meta surface and introducing shorting pin series on the edge, the design gave a wide impedance bandwidth ranging from 4.3-5.4GHz with a peak gain of 9.8dBi. Additionally, a meta surface antenna provided by a slot feeding architecture incorporating capacitive loading strips in a four-element truncated patch array showed further gain improvement with an overall peak gain of 11 dBi compared to traditional designs[35][36][37].

Despite great efforts in the design of wearable antennae for both RF identification (RFID) and Wi-Fi, a small, high-gain, and electrically efficient antenna operating at microwave frequencies in a stable manner is a difficult problem to solve. Many existing wearable antennas have relied on textile or polymer-based substrates to provide looseness of fit; however, they have high dielectric losses, unstable permittivity, sensitivity to moisture, and performance degradation on bending the antenna, especially in the 5 - 6 GHz region. On the other hand, traditional rigid antennas designed on low-loss substrates have good electrical performance, but lack conformability and cannot be used in wearable and space-limited scenarios. Furthermore, existing miniaturization techniques often lead to loss of gain, narrow bandwidth, or polarization quality, which limits their suitability for the systems of the radio frequency identification (RFID) or wireless local area network (WLAN) technology, which requires robust and orientation-insensitive communication. Therefore, there is an obvious need for an antenna design that can address the miniaturization, gain enhancement, and mechanical adaptability, and at the same time guarantee stable performance at the targeted microwave band. This work tries to bridge this gap by presenting a flexible, shorting pin integrated patch antenna that addresses limitations of current wearables: (1) Radio Frequency Identification (RFID) and (2) Wireless Local Area Network (WLAN) antennas design.

To add to the projected design research in wearable antenna design, this paper aims to provide the design and analysis of a wearable antenna with a micro microstrip structure, which carries a rectangular patch shape with single-band, resonating waves of 5.7 GHz for IoT and wearable RFID applications. The frequency band 5.7 GHz is of specific importance in today's wireless communication and applications based on the Internet of Things (IoT) that use radios with radio-frequency identification (RFIs) for communication over short distances. 5.7 GHz is globally available in the ISM (Industrial, Scientific, and Medical) frequency spectrum and therefore can be used in an unlicensed manner under the regulations of most regions. This

frequency provides a good compromise between the size of the antennas, bandwidth, and propagation characteristics and allows for the design of small and high-performance antennas that are suitable for portable and space-constrained devices. Moreover, there are also many modern UWB, RFI, and IoT systems that are based on or around this band and are thus highly relevant for both research and practical deployment. By focusing on the 5.7 GHz, antennas can be used for reliable communication, good coverage, and effective integration into modern wireless systems (collaborating to bring next-generation IoT and RFID technologies to fruition) while representing an important link in the advancement of ongoing technologies and IoT advancements[38][39]. The antenna is designed on a flexible Rogers RT/Duroid 5880 substrate, making it suitable for wearable use. It shows good radiation features as well as competitive gain performance, efficiency performance, bandwidth performance, and reflection coefficient performance. Furthermore, the evaluation of the specific absorption rate (SAR) is fundamental in the comprehension of electromagnetic wave-tissue interactions, which is a crucial key for the assessment of antenna wearability and the safety of the user. Accordingly, SAR analysis is carried out using a two-layer tissue phantom, and the results show that there is compliance and satisfactory performance in the desired operating frequency.

### **Antenna Configuration:**

### **Methods and Materials:**

The antenna was designed and simulated with CST Studio Suite using Rogers RT5880 (Rogers Corporation, Chandler, AZ, USA) with a relative permittivity of 2.2 and a dielectric loss tangent value of 0.0009. Rogers RT5880 offers the advantage of having very low electrical loss, very low moisture absorption, isotropic properties used in all directions, and stable electrical characteristics over a wide frequency range, in addition to having a high degree of chemical resistance. Owing to its high flexibility, this substrate has become a suitable choice for modern IoT and wearable device applications, where there is a need for mechanical adaptability. Moreover, recent research efforts on flexible RFID technologies have been using Rogers RT5880 with increasing frequency since it is easy to fabricate and its performance is reliable under bending conditions[40][41][42].

### **Initiating Antenna Design:**

The first part of the proposed work dealt with the development of the radiating patch on the basis of the fundamental principles of microstrip patch antenna design. This process started with identifying fundamental parameters, like patch dimensions, substrate properties, and operating frequency, that have been found using well-established analytical formulae. These initial calculations formed a basis for the definition of the physical geometry of the antenna in order to ensure proper resonant behavior and desirable radiation characteristics. The design of this proposed antenna is based on the standard microstrip patch antenna equations that calculate the important dimensions of the patch antenna and its important parameters for predictable and repeatable resonant behavior. The patch length and width are calculated on the basis of the intended operating frequency, substrate dielectric constant, and substrate thickness, taking into consideration equations for effective dielectric constant and extended patch length to take fringing effects into consideration. Feed position is calculated to achieve proper impedance matching, and other parameters like slots or shorting pins are added depending on their effect on resonance and bandwidth. By systematically applying these known formulas, the dimensions of the antenna are determined according to the target frequency band and allow to accurately control of the resonance frequency, impedance, and radiation characteristics while ensuring a compact, efficient design of the antenna. By using the classical theoretical model of microstrip antennas as a basis, the actual design was laid, and a good basis for building a simple initial prototype was laid, which was further improved by advanced modifications and optimization[43][44][45].

$$W = \frac{v_0}{2f_r} \sqrt{\frac{2}{1 + \epsilon_r}} \#(1)$$

$$L = \frac{v_0}{2f_r \sqrt{\epsilon_{ref}} - 2\Delta L} \#(2)$$

$$\epsilon_{ref} = \frac{\epsilon_r + 1}{2} + \frac{\epsilon_r - 1}{2} \left[ 1 + 10 \frac{h}{W} \right]^{-\frac{1}{2}} \#(3)$$

$$\Delta L = 0.412h \frac{(\epsilon_{ref} + 0.3) \left( \frac{W}{h} + 0.264 \right)}{(\epsilon_{ref} - 0.258) \left( \frac{W}{h} + 0.8 \right)} \#(4)$$

Here, W and L represent the width and the length of the radiating patch, and  $\epsilon_{ref}$  represents the effective dielectric constant.  $\Delta L$  shows the increase in the effective length of the radiating patch due to the fringing effect. In the given context,  $f_r$  represents the operating frequency,  $\epsilon_r$  is the dielectric constant of the substrate,  $v_0$  is the speed of light. The dimensions of the ground plane for the patch antenna can be determined by the following equations (5) and (6).

$$L_g = L + 6 \times h \#(5)$$

$$W_g = W + 6 \times h \#(6)$$

### Design Progression:

Miniaturization plays an important part in the design of antennas today. It is supposed to minimize the physical size of the antenna, decrease the footprint, increase cost-effectiveness, and increase comfort, especially for biomedical applications, wearable applications, and also for the range of radio frequency identification (RFID) applications. Conventionally, the size of the microstrip antenna is about half the wavelength at its resonating frequency. For example, at the resonance frequency of 1 GHz, the ideal antenna length would be around 100 mm. Such dimensions are usually impractical for compact and wearable systems, for which size constraints are very stringent. To overcome this problem, various miniaturization schemes have been studied in the design of microstrip patch antennas by adding, for instance, the use of slots, high-frequency shorting pins, loading materials, fractals, high permittivity substrates, pin shortening schemes, and the use of metamaterials. These concepts typically work by adding length to a current path, and so increase the electrical length of an antenna, without affecting its actual size. Following this principle, the present work uses rectangular-shaped slots in a conventional rectangular patch to effect good miniaturization [46].

The proposed antenna geometry is shown in Figure 2, where Figure 2(a) represents the top view of the corresponding radiating patch, and Figure 2(b) is the back view and indicates the ground plane configuration. The radiating patch is etched on a Rogers RT5880 substrate and contains two accurately dimensioned rectangular slots of  $8 \times 1 \text{ mm}^2$  and  $6 \times 1 \text{ mm}^2$ , introduced to increase the path length of surface current and thus to tune the resonant frequency, and gives part of the miniaturization aspect. Within the top view, the two red markers are the locations of the shorting pin and the probe feed, the shorting pin also gives an alternative path for the current to return, which effectively decreases the operating frequency, without enlarging the physical dimension of the antenna, the probe feed is located to obtain optimum impedance match and efficient excitation of the desired resonance mode. On the underside, the antenna uses a full ground plane for stable radiation characteristics and no unwanted back radiation, but has two rectangular slots with a size of  $6.4 \times 2.6 \text{ mm}^2$  for modification of the ground plane current distribution to contribute to the desired resonant behavior for better impedance characteristics. Together, with patch slots plus shorting pin

integration, plus feed positioning, plus ground plane shaping, a consolidated design approach that is suitable for controlling the resonance, physically reducing the size, and improving the electrode resonance of the antenna.

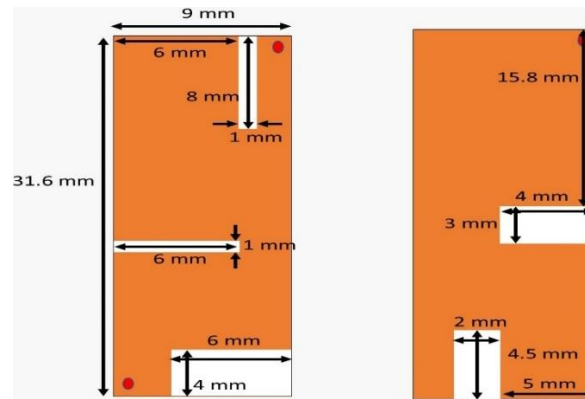


**Figure 2.** Geometry of the Proposed Antenna (a)Top View (b) Bottom View

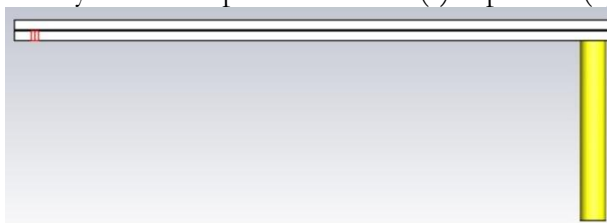


**Figure 3.** Probe-Feed and Shorting Pin Side View

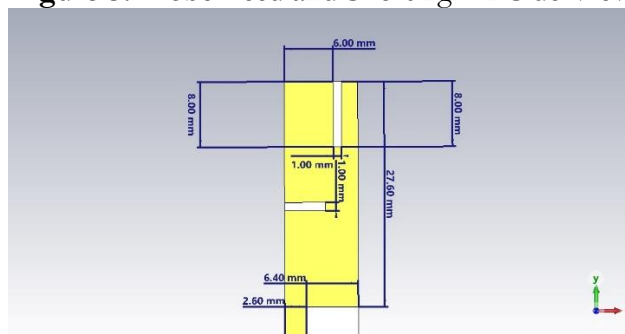


**Figure 4.** Post Optimization Dimensions of the Proposed Design

A systematic design of antenna geometry by a parametric analysis instead of an automated global optimization algorithm has been applied. Key design parameters, such as patch length and width, slot dimensions, feed position, and shorting pin positions, were varied uniquely and incrementally to assess the impact of the design parameters on the antenna's operational frequency, impedance matching degree, axial ratio, and realized gain. The optimization process was intended to reach  $|S_{11}|$  less than or equal to -10 dB at the target frequency of 5.7 GHz and maximum gain within the limit of antenna miniaturization as well as mechanical flexibility. This was assumed to have converged when changes in these parameters caused a negligible change in performance measures. This step-by-step parametric approach affords a clear physical insight into the role of each design parameter whilst ensuring a reproducible and reliable path in the design of the optimized antenna configuration. The optimization of the antenna geometry is done with the objective of getting better radiating results while being stable and consistent in terms of resonant frequencies across the desired operating band. This process includes the systematic fine adjustment of the critical structural parameters about dimensions of the radiating-patch, thickness, and dielectric properties of the substrate, feed mechanism's positioning and configuration, etc. By adjusting these parameters through iterations, the effective current distribution on both the patch and ground plane can

be adjusted, allowing goal improvements in impedance matching, gain, bandwidth, and overall radiation and efficiency to be achieved. In addition, careful optimization is required to guarantee that the antenna will still have the desired resonance properties even after introducing miniaturization features such as slots and shorting elements, and thus be robust enough to still maintain performance while reducing physical dimensions.

### Analysis of the Simulated Outcomes:

The antenna design is first performed and simulated to verify the electromagnetic behavior of the antenna and to make sure that the designed antenna structure meets the desired performance requirements. Throughout the design process, parametric sweeps are performed where important geometric parameters (e.g., slot dimensions, feed position, substrate thickness) are systematically varied in order to observe the effect on resonant frequency, impedance matching, and radiation characteristics. These iterative evaluations provide the freedom to identify the critical design sensitivities and performance trends. In addition to parametric analysis, advanced optimization techniques available in the simulation environment are used to perform automatic fine-tuning of the antenna geometry with a view to automatically converging towards a good solution. Through this combined approach of manual parameter exploration and algorithm-driven optimization, the resulting design has better radiation efficiency, consistent resonance, and well-matched impedance characteristics.

### Reflection Coefficient:

Figure 5 shows the simulated results of the reflection coefficient ( $S_{11}$ ) of the proposed antenna. The analysis shows that the return loss is consistently less than -10 dB across the targeted frequency band, and thus impedance matching is effective, and little power is reflected. These results confirm the validity of the design and optimization process by attesting to the efficient radiation of the input power by the antenna over the desired operating frequencies. In addition to this, the reflection coefficient trend gives information about the resonant behavior, bandwidth, and overall stability of the antenna under the simulated condition.

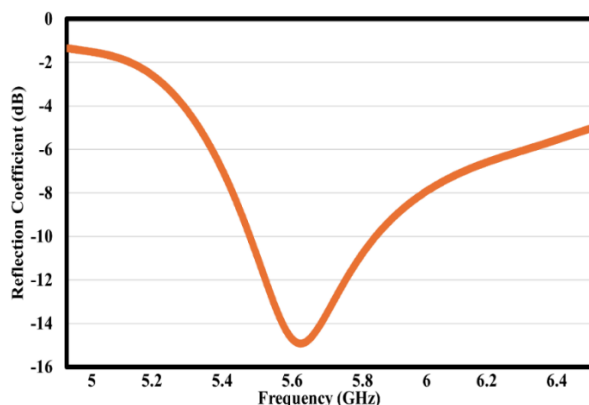


**Figure 5.** Reflection Coefficient of the Proposed Antenna

Based on the reflection coefficient ( $|S_{11}|$ ) analysis, the antenna has an impedance bandwidth = 40 MHz using the -10 dB reflection coefficient criterion. This represents a percentage bandwidth of 6.5%, showing that there is adequate impedance matching over the operating frequency range.

In the proposed antenna design, the shorting pins and slots are arranged appropriately to accommodate the control of the resonant frequency as well as impedance matching. The shorting pins provide capacitive coupling between the radiating patch and the ground plane, essentially lowering the resonant frequency and thus allowing for the miniaturization of the antenna without having a major effect on the efficiency of radiation. The slots, on the other hand, are used to adjust the distribution of current on the patch, which permits fine-tuning of the resonance as well as the axial ratio for polarization. A parametric study was performed, in

which the parameters, such as the pin positions, diameters, and slot lengths, were varied, which showed a direct effect on the resonant frequency and bandwidth. The use of this systematic approach makes the rationale behind the chosen configuration pretty clear, allowing the reproducibility as well as optimized performance of the suggested antenna to be achieved. Figure 3 represents the parametric analysis of the antenna with and without a shorting pin. Without the shorting pin, the resonance frequency shifted to the right, and the design is unable to achieve the desired band as shown in Figures 6 and 7.

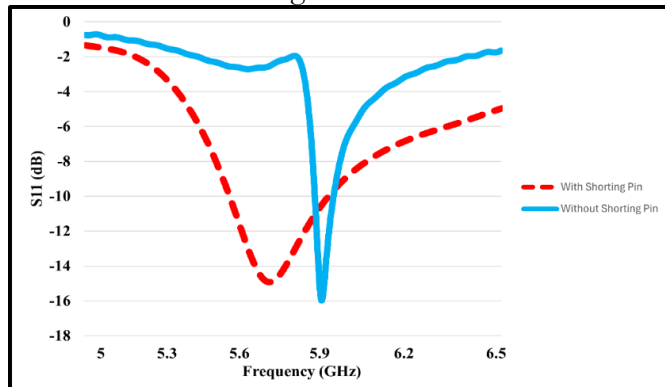


**Figure 6.** Parametric Analysis of With and Without Shorting Pin

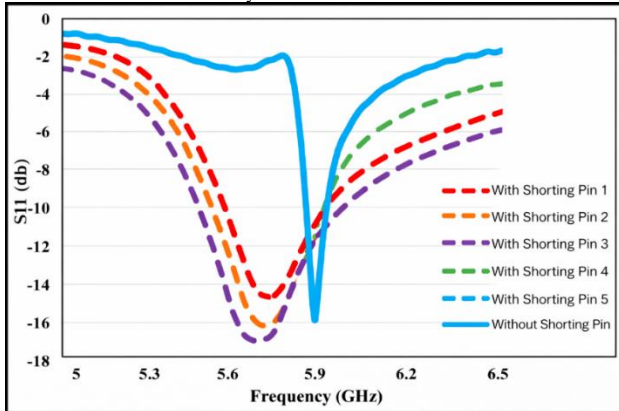


**Figure 7.** Parametric Study with Different Positions of Shorting Pin  
Radiation Pattern:

Figures 8 and 9 show the 2D and 3D radiation patterns for the proposed antenna on an operating frequency of 5.7 GHz, emulated in three dimensions (3-D) to provide a complete vision of its radiation behavior in space by integrating the azimuth plane ( $\nu = 0^\circ$ ) and elevation plane ( $\nu = 90^\circ$ ). The findings suggest that the antenna has improved directionality in the E-plane (i.e., with a value of  $f$ , or  $f = 0^\circ$ ) in which the main lobe is more focused and pronounced, meaning there is a more concentrated radiation in this plane and a relatively wider and less directional radiation distribution in the H-plane (i.e., with a value of  $f$ , or  $i = 90^\circ$ ). Additionally, a clearly seen bidirectional radiation characteristic at  $\theta = 90^\circ$ , this suggests symmetrical radiation in opposite directions, consistent with the physical structure and desired operation characteristics of the antenna. The figure further shows a good consistency of the simulated radiation pattern with the measured radiation pattern with respect to the main lobe directions and similar radiation intensities, thus proving the correctness of the simulation model as well as the reliability of the experimental validation. Moreover, the high correlation between the 3-D radiation pattern and corresponding two-dimensional (2-D) radiation cuts can be observed, which could provide more proof of consistency and robustness of the radiation performance at varying planes of observation.

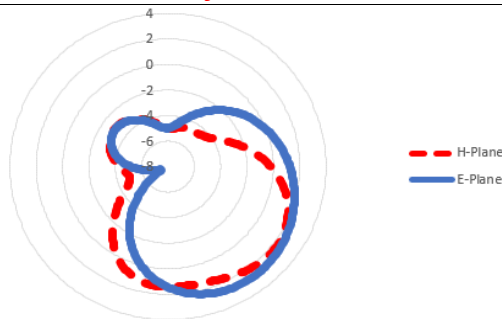


**Figure 8.** Illustration of Radiation Pattern for E and H-plane at 5.7 GHz

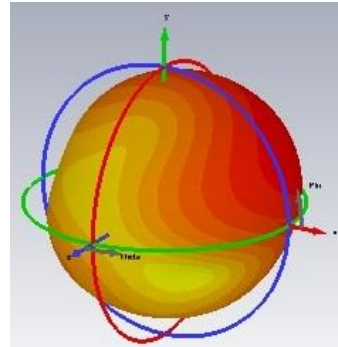


**Figure 9.** 3D Radiation Pattern of the Proposed Antenna

Here, the front-to-back ratio or F/B of the proposed wearable antenna is examined from the simulated 3D radiation patterns. The maximum F/B ratio at operating frequency is found to be about -0.5 dB, showing that the antenna is radiating mainly in the forward direction, such that it is very little in the backward direction and towards the body. This characteristic is especially beneficial for wearable applications, as a reduced amount of energy is absorbed in the human body, which increases radiation efficiency in the desired direction.

The polarization purity of the antenna is measured by the co-polarization and cross-polarization components of the field radiated by the antenna. The cross-polarization levels are found to be -2 dB, and the main lobe gives a high polarization purity of approximately 61.5 %. This verifies that the antenna has a mostly linear polarization at the operating frequency, which is very necessary to minimize polarization mismatch and ensure reliable wireless communications.

#### Efficiency and Gain:

Antenna efficiency is a major parameter that measures the ratio of input power delivered to the antenna relative to radiated electromagnetic energy and hence the number of losses in the antenna structure. It is a good measure of the antenna's ability to operate with low levels of dissipation caused by such factors as conductor losses, dielectric losses, and impedance mismatch. A greater efficiency indicates that more of the input power is successfully radiated to free space to transmit a signal or successfully captured at reception, while a lesser efficiency means that a large amount of power is being wasted as heat or lost through some other non-radiative process. Consequently, high antenna efficiency is necessary to improve the overall performance of the system, reliability of communication, operational range, and avoid unneeded consumption of energy. As shown in Figure 7, the radiation efficiency of the proposed antenna reaches around 82.5% at the operating frequency of 5.7 GHz, which proves its suitability for efficient and reliable wireless communication applications.

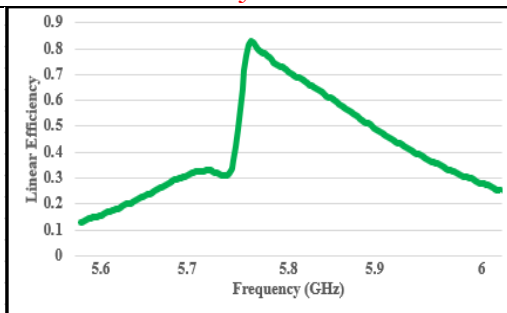


**Figure 10.** Linear Efficiency of the Proposed Design

Antenna gain is one of the key performance figures of the antenna that characterizes the ability of the antenna to focus radiated power in a specific direction with reference to an isotropic radiator. It is an amalgamation of the directivity and efficiency of the antenna and thus tells how well the antenna can transmit or receive signals in the desired direction. A higher gain simply means better signal radiation and better reception capability, which is especially true for wireless communication systems where improved signal strength, coverage, and reduced signal interference are desirable. Figure 10 presents the gain characteristics of the proposed antenna, from which it is clear that the antenna has a maximum gain of about 4.1 dBi at the operating frequency of 5.7 GHz, proving the antenna can be used in reliable and efficient directional communications applications.

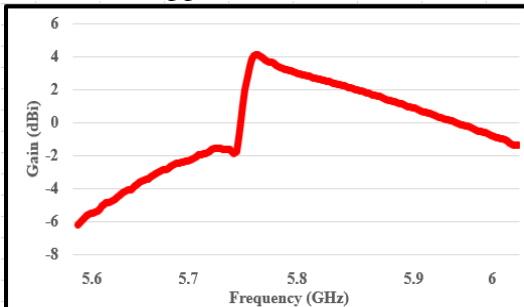


**Figure 11.** Gain Profile of the Proposed Antenna

The radiation efficiency and the realized gain of the proposed wearable antenna are compared with wearable and body-centric antennas that have been reported recently and that operate in similar frequency bands. As shown in Table 1, the proposed design exhibits excellent competitive performance with higher efficiency, although its size is small and conformal design. While a few of the antennas that are reported have slightly increased gain, they tend to be based on larger ground planes, rigid substrates, or thicker profiles, and therefore, their use in a practical wearable application is limited. In contrast, the proposed antenna is stable gain-throughput under on body condition while providing superior flexibility and reduction of the profile thickness. These results show that the proposed antenna offers a good trade-off between efficiency, gain, and wearability, which is suitable for on-body wireless communication systems.

**Table 1.** Comparison of the Efficiency and Gain Profile of the Proposed Antenna

Reference	Frequency Band	Gain (dBi)	Efficiency
[47]	5.7 GHz	3.9	74%
[48]	5.7 GHz	3.1	60%
[49]	5.7 GHz	2.9	48.9%
[50]	5.7 GHz	3.2	72%
This Work	5.7 GHz	4.1	82%

**Surface Current Distribution:** The resonance condition allows the best energy transfer to occur between the antenna and the surrounding medium. The surface current distribution,

which is a representation of the flow of electric current over the antenna structure, is an important factor in obtaining resonance. As shown in Figure 12, the surface current distributions at the resonant bands reveal information in regard to the current flow patterns on the antenna at different operating frequencies. Variations in these current distributions allow the antenna to efficiently resonate and maintain efficient performance over a number of frequency ranges by using the same excitation at the input port.

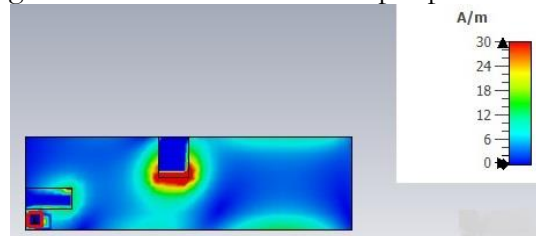


**Figure 12.** Distribution of Surface Current

At the lower operating frequency of 5.7 GHz, due to the antenna, the surface current takes a longer path on the periphery of the radiating patch. As the frequency of operation is raised, a definite concentration of surface current can be seen towards the center region of the antenna. This behavior can be attributed to high-frequency effects such as increased current confinement. As the path length of effective current is reduced at higher frequencies, the antenna will show two states of resonance at higher bands, reinforcing the well-known principle that a low effective antenna size means that its resonant frequency is high. Also, the resonant frequency can be deduced based on the effective length of the path of surface current on the radiating patch. Ideally, resonance will occur when the effective electrical length is about one-half a wavelength. In structures of printed antennas, the medium of radiation is considered to be almost equally split between the medium of the substrate and air.

When trying to design flexible or conformal antennas, it is important that the right substrate is chosen as it requires a balance between mechanical flexibility and electrical characteristics. Compared with fully flexible materials such as PDMS, silicone, or textile-based substrates, Rogers RT/5880 has a better dielectric stability, Low loss tangent, and consistent permittivity, which is very important in high-frequency microwave and millimeter wave applications. While PDMS/materials already offer good bending/conformability, higher dielectric losses through variable material properties and reduced dimensional stability can result in antenna efficacy/radiation performance. Thin-core RT/5880, on the other hand, can allow moderate bending while retaining the high gain, wide bandwidth, and predictable impedance characteristics needed for the reliability of reliable wireless communication. Additionally, when laminated with flexible backing materials, RT/5880 can not only obtain mechanical flexibility but also high electrical performance, which is extremely suitable for flexible and wearable antenna design, where both requirements are needed to be satisfied. Although regular RT/5880 laminates are rigid and can't be bent, thin-core versions of RT/5880 have adequate mechanical flexibility for use in some low curvature applications. By decreasing the thickness of the substrate (e.g., to 0.254-0.305 mm), there is a limit for the laminate to bend without cracking or delamination, and it is possible to have conformal or semi-flexible antenna structures. This flexibility allows the design of miniaturized and very low-loss and high-gain performance microwave antennas, which can be integrated in curved surfaces or platforms that can be worn, while preserving the excellent dielectric properties (low loss tangent and stable dielectric constant) of RT/5880. Furthermore, thin-core RT/5880 can be used in combination with flexible backing material such as PET or silicone to improve mechanical robustness so that it can be used as a substrate for flexible and semi-conformal applications for IoT or wearable and bodily area network systems. Figure 13 shows the almost

same surface current distribution in the bent condition as in the flat form that proves the flexibility in the material.

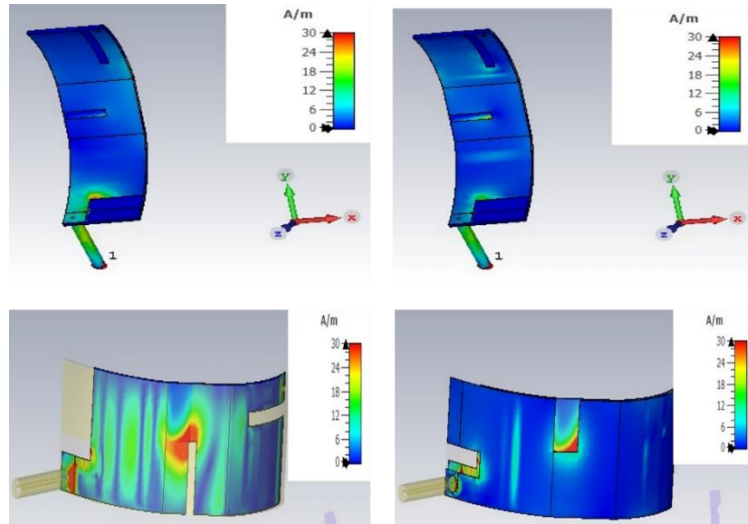


**Figure 13. Surface Current Distribution in Bent Condition**

Table 1 shows a comparison of this work with the other state-of-the-art existing work in connection with the bending properties.

**Table 2.** Comparison of the Work with Existing Literature

Reference	Frequency Band	Substrate Material	Flexibility	Bending Tolerance	Comfort and Wearability
[21]	2.4 GHz	Rogers RT5880 (Thick Core)	Moderate	Up to 40% Deformation	Lightweight, skin-friendly substrate
[51]	5.85 GHz	Wool Paper	High	Up to 25% Deformation	Comfortable for daily wear
[52]	2.45 GHz	Denim	High	Up to 35% Deformation	Lightweight, skin-friendly substrate
[53]	3.5 GHz	Textile	High	Up to 30% Deformation	Breathable, suitable for sportswear
[54]	5.035 GHz	Denim	High	Up to 35% Deformation	Lightweight, skin-friendly substrate
[55]	6 GHz	Textile	High	Up to 30% Deformation	Breathable, suitable for sportswear
[56]	5.78	Rogers RT5880 (Thick Core)	Low	Up to 40% Deformation	Lightweight, skin-friendly substrate
This Work	5.7 GHz	Rogers RT5880 (Thin Core)	High	Up to 20% Deformation	Excellent skin conformity

#### SAR Analysis:

Specific absorption rate (SAR) analysis is required for wearable devices to measure the amount of electromagnetic energy absorbed by the surrounding biological tissues.

$$SAR = \frac{\sigma E^2}{2\rho} \#(7)$$

Equation (7) gives the SAR in units of W/kg, where E is the electric field vector (V/m), sigma (S/m) is the effective conductivity, and rho is the density of the tissue layers. The model considers tissue thicknesses of 40 mm for muscle, 2 mm for fat, and 1 mm for skin, with densities of 1020 kg/m<sup>3</sup>, 909 kg/m<sup>3</sup>, and 1060 kg/m<sup>3</sup>, respectively. The dielectric properties of these layers were characterized using the second-order Debye model, which could accurately capture the frequency-dependent dispersion effects[57].

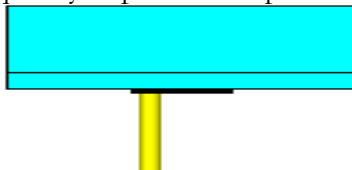


**Figure 14.** Antenna Placed on Phantom

A comparison of the reflection coefficient of the antenna in free space and on a tissue phantom is shown in Figure 15. The results agree closely with each other, with a very small frequency shift. This slight drift is to be expected because antennas will show a changed behavior when loaded by a dispersive medium such as biological tissue. The effect of this loading is clear from the detected change in the reflection coefficient, as is shown in Figure 15.

The Specific Absorption Rate (SAR) analysis of the proposed wearable antenna is performed based on a two-layer human tissue phantom model in order to represent the on-body operating conditions realistically, as shown in Figure 14. The phantom is made up of layers of skin and muscle with a mass density of 1010 kg/m<sup>3</sup>, consistent with commonly employed values used in the evaluation of wearable antennas. SAR simulation is performed at the operating frequency of the antenna at an input power of 8 mW. Figure 15 shows the simulated distribution of the SAR and the corresponding peak SAR averaged over 1 g of tissue. The maximum SAR<sub>1g</sub> value is found to be 0.808 W/kg, which is well below the limit of 1.6 W/kg of the Federal Communications Commission (FCC) guidelines for an uncontrolled environment. These results validate the proposed antenna to meet the safety requirements and mandatory regulations, and are applicable for use as wearable and on-body wireless communication applications.

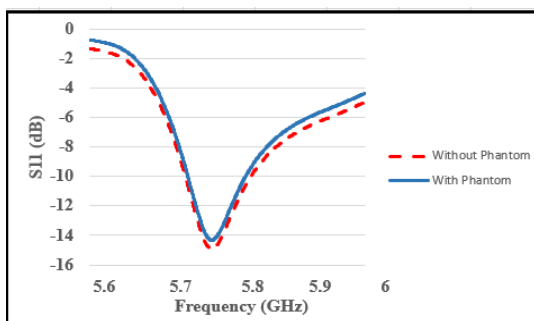


**Figure 15.** Antenna's Performance with and without Phantom

### Result and Discussion:

This work presents the comprehensive design and analysis of the development of a compact single-band wearable antenna using the CST Microwave Studio simulation environment. Antenna miniaturization is realized by the integration technology that implements a shorting pin and sensible slotting of the radiating element, which provides the strength to significantly reduce the physical dimension while allowing good impedance matching and an adequate operational bandwidth for the presence at the desired resonant frequency. The proposed antenna is designed for applications in WLAN, Internet of Things

(IoT), and wearable RF identification, where it is important to have a small size, high efficiency, and stability.

Both numerical computation and complete wave electromagnetic simulations are used to exhaustively evaluate key performance metrics such as reflection coefficient, radiation patterns, radiation efficiency, and realized gain. The simulated results show that the antenna behaves stably with properly maintained radiation characteristics, and it can be considered that the antenna performance in the above-mentioned designed operating conditions is reliable. In addition, surface current density distributions are analyzed at the resonant frequency to provide physical insight into the operation of the antenna, pointing out the role played by the shorting pin and slot geometry in the control of current paths and in the miniaturization and resonance tuning of the antenna.

To ensure wearability and user safety, phantom modeling is implemented to simulate the realistic condition on the body. A thorough analysis of SAR is done to quantify the electromagnetic energy absorption due to the interaction of tissues with waves operating at its frequency. The derived SAR values are indicated to the learner, the regulatory safety boundary of 1.6 W/kg as specified by the Federal Communications Commission (FCC), indicating that the proposed antenna is safe for wearable applications. Overall, the results validate the effectiveness of the proposed design in achieving a favorable trade-off between compact size, electrical performance, and user safety for the body-centric wireless communication systems.

For future work, attempts will be made to improve the wearability of the antennas by using substrates made of highly flexible materials like polyfoam, jeans, or denim. Fractal-type designs might help other miniaturization even more, multiple elements array configurations or MIMO (multiple inputs, multiple outputs) implementation might be more suitable for gain, data throughput, and reliability. These strategies are working to improve the performance, versatility, and functionality of the antenna as a whole through the use of advanced materials, complex geometries, and advanced configurations. It must be noted that the mentioned results in this study are solely on the basis of full-wave electromagnetic simulations, and no physical prototype fabrication and experimental measurements have been made at this point. While analysis using simulation is a good basis to understand the resonance behavior of the antenna, the radiation characteristics, and the parametric sensitivity, experimental validation is necessary to thoroughly understand practical aspects, such as fabrication tolerance, material imperfection, connector losses, or environmental effects such as bending or proxing human body. These factors may create shortcuts between simulation and real-life performance. Therefore, in the future, the aim will be to build a physical prototype for the proposed antenna and undertake complete experimental characterization, including measuring S-parameters, radiation pattern, gain measurement, and bending tests under real wearable conditions. Such validation would further confirm the feasibility and reliability of the proposed design for practical applications of the proposed technologies for use in RFID, ISM, and wearable biomedical applications.

Although the proposed wearable antenna achieves enough performance, several aspects can be further improved in future studies. First, while acceptable radiation efficiency and gain are realized, performance degradation is observed under conditions of severe bending and close on-body placement. Future works will be performed in the direction of structural optimization and the use of sophisticated flexible or meta surface-based substrate for the improvement of radiation characteristics under dynamic wearable situations.

Secondly, although the present design meets FCC requirements for SAR in low input power levels, it is desirable for the SAR to be further reduced, especially for high transmit power and for long on-body operation. Future investigations will look into the use of electromagnetic bandgap (EBG) structures, artificial magnetic conductors (AMC), or shielding layers to reduce the backward radiation and reduce the energy absorption in human tissues.

Lastly, the currently used antenna only works in one frequency range. To further the versatility for the upcoming field of wearable and body-centric communication systems, future research will focus on expanding the design into multiband and reconfigurable operation using approaches such as slot loading, switchable elements, or tunable materials, while preserving compactness and flexibility in the design, including safety for the users.

### Conclusion:

In this study, the design and analysis of a miniaturized flexible patch antenna with shorting pin integration for applications in radio frequency identification (RFID), industrial, scientific, and medical (ISM), and wearable biomedical systems are presented. By utilizing shorting pins and optimized slot structure, the antenna can realize large size reduction, combined with high performance, which solves the design problems of space-constrained and wear-composed environments. The antenna structure is designed on a thin-core Rogers RT/5880 substrate, which has the characteristics of mechanical flexibility (can be bent moderately without affecting the electrical performance), low dielectric loss, stable permittivity, and consistent gain, which is better than the textile-based traditional flexible substrate. Simulation results show that the antenna has a resonance frequency of 5.7 GHz with a reduced dimension that is good for integration into portable devices, and also shows a peak gain improvement over standard patch design. Furthermore, the antenna has a broad beam width and ensures reliable communication in different orientations, which is especially useful in wearable and biomedical telemetry applications.

Overall, the proposed antenna design yields a balance of good miniaturization, high radiation efficiency, and mechanical flexibility, and is especially good for integration with wearable and body-centric wireless applications. Condition of careful use of shorting pins, slotting techniques allow realizing this compact footprint without any trade-offs regarding impedance matching and bandwidth, ensuring stable and reliable performance across the desired operating frequencies. Its high efficiency and consistent radiation features make it a stable solution for the next-generation application, such as in the field of radio frequency identification (RFID). The ISM frequency (RF) band is also used in the wireless field, such as a usable wireless network. Beyond these immediate applications, the design provides a firm foundation for future experimental validation (prototype fabrication and on-body testing), as well as being necessary for any practical deployment in Internet of Things (IoT) circumstances, as well as biomedical monitoring situations. The combination of electrical performance, wearability and Safety compliance with SAR regulations proposed by this antenna presents the potential to achieve the stringent requirements of modern wireless communication systems while opening an avenue for further optimization and multifunctional integration of the antenna.

**Acknowledgement:** The authors would like to acknowledge the support provided by their respective institutions for facilitating this research. The authors also thank the developers of the CST Microwave Studio software for providing the simulation tools used in this work.

**Author's Contribution:** **Waqas Ali:** Conceptualization, antenna design, simulation studies, and drafting of the manuscript. **Nizam-Ud-Din:** Supervision, review, and editing of the manuscript. **Muhammad Zahid:** Data analysis, interpretation of results.

**Conflict of interest:** The authors declare no conflict of interest in publishing this manuscript in IJIST.

**Project details:** No external funding was received for this research.

### References:

- [1] “8.4 Billion Connected Things Will be in Use 2017 | Gartner.” Accessed: Dec. 24, 2025. [Online]. Available: <https://www.gartner.com/en/newsroom/press-releases/2017-02-07-gartner-says-8-billion-connected-things-will-be-in-use-in-2017-up-31-percent-from-2016>

[2] K. V. S. Rao, P. V. Nikitin, and S. F. Lam, "Antenna design for UHF RFID tags: A review and a practical application," *IEEE Trans. Antennas Propag.*, vol. 53, no. 12, pp. 3870–3876, Dec. 2005, doi: 10.1109/TAP.2005.859919.

[3] C. Sun, Z. Wu, and B. Bai, "A Novel Compact Wideband Patch Antenna for GNSS Application," *IEEE Trans. Antennas Propag.*, vol. 65, no. 12, pp. 7334–7339, 2017, doi: 10.1109/TAP.2017.2761987.

[4] J. Ren, H. Liu, Y. Zeng, Z. Wang, and S. Fang, "Dual-Band Circularly Polarized Antenna with Wide Axial-Ratio and Gain Beamwidths for High-Precision BDS Applications," *Prog. Electromagn. Res. C*, vol. 145, pp. 63–74, 2024, doi: 10.2528/PIERC24052202.

[5] K. Wei *et al.*, "A Dual-Band Rotational Feed Circularly Polarized RFID Reader Antenna Array With Stable Gain," *IEEE Antennas Wirel. Propag. Lett.*, vol. 24, no. 7, pp. 1620–1624, 2025, doi: 10.1109/LAWP.2025.3543388.

[6] S. Chenaoui, L. Mouffok, S. Hebib, A. Fattouche, D. Allane, and S. Tedjini, "Gain stability improvement of a wideband antenna using an artificial magnetic conductor," *Microw. Opt. Technol. Lett.*, vol. 65, no. 8, pp. 2267–2277, Aug. 2023, doi: <https://doi.org/10.1002/mop.33673>

[7] T. Lou, Z. Shen, and X. X. Yang, "Circularly Polarized UWB Antenna Based on a Single-Folded Substrate," *IEEE Antennas Wirel. Propag. Lett.*, vol. 23, no. 7, pp. 2195–2199, 2024, doi: 10.1109/LAWP.2024.3384979.

[8] X. Liu, Y. Zhu, and W. Xie, "A Miniaturized Wideband Directional Circularly Polarized Antenna Based on Bent Vivaldi Antenna Structure," *IEEE Antennas Wirel. Propag. Lett.*, vol. 22, no. 2, pp. 298–302, Feb. 2023, doi: 10.1109/LAWP.2022.3209611.

[9] H. Yang *et al.*, "Aperture Reduction Using Downward and Upward Bending Arms for Dual-Polarized Quadruple-Folded-Dipole Antennas," *IEEE Antennas Wirel. Propag. Lett.*, vol. 22, no. 3, pp. 645–649, Mar. 2023, doi: 10.1109/LAWP.2022.3221468.

[10] P. V. Nikitin and K. V. S. Rao, "Antennas and propagation in UHF RFID systems," *2008 IEEE Int. Conf. RFID (Frequency Identification)*, IEEE RFID 2008, pp. 277–288, 2008, doi: 10.1109/RFID.2008.4519368.

[11] G. Marrocco, "The art of UHF RFID antenna design: Impedance-matching and size-reduction techniques," *IEEE Antennas Propag. Mag.*, vol. 50, no. 1, pp. 66–79, Feb. 2008, doi: 10.1109/MAP.2008.4494504.

[12] "(PDF) UHF RFID antenna architectures and applications." Accessed: Dec. 24, 2025. [Online]. Available: [https://www.researchgate.net/publication/266583117\\_UHF\\_RFID\\_antenna\\_architectures\\_and\\_applications](https://www.researchgate.net/publication/266583117_UHF_RFID_antenna_architectures_and_applications)

[13] D. Zhao, Y. Z. Yin, and Y. Yang, "A review of antenna design and measurement for UHF RFID tags," *2010 9th Int. Symp. Antennas Propag. EM Theory, ISAPE 2010*, pp. 349–352, 2010, doi: 10.1109/ISAPE.2010.5696472.

[14] J. Zhang, G. Y. Tian, A. M. J. Marindra, A. I. Sunny, and A. B. Zhao, "A Review of Passive RFID Tag Antenna-Based Sensors and Systems for Structural Health Monitoring Applications," *Sensors 2017, Vol. 17, Page 265*, vol. 17, no. 2, p. 265, Jan. 2017, doi: 10.3390/S17020265.

[15] J. Ghalibafan and F. H. Kashani, "A circularly polarized fractal microstrip antenna for RFID applications," *2009 IEEE Int. Symp. Radio-Frequency Integr. Technol. RFIT 2009*, pp. 319–322, 2009, doi: 10.1109/RFIT.2009.5383721.

[16] P. Charoenchue, C. Phongcharoenpanich, K. Phaebua, and K. Aunchaleevarapan, "A circularly polarized square plate antenna with two inclined slots for UHF-RFID reader," *2011 Int. Symp. Intell. Signal Process. Commun. Syst. "The Decad. Intell. Green Signal*

Process. *Commun. ISPACS 2011*, 2011, doi: 10.1109/ISPACS.2011.6146137.

[17] K. S. Rana and D. S. Ajij, “Design and simulation of NFC printed antenna in near field wireless communication for SDC,” *2016 IEEE Int. Conf. Distrib. Comput. VLSI, Electr. Circuits Robot. Discov. 2016 - Proc.*, pp. 247–251, 2016, doi: 10.1109/DISCOVER.2016.7806249.

[18] Y. Li, S. Sun, L. Jiang, and T. T. Ye, “A circular polarization hybrid-integrated rectangular ring antenna for RFID reader,” *IEEE Antennas Propag. Soc. AP-S Int. Symp.*, 2012, doi: 10.1109/APS.2012.6349197.

[19] S. C. Lin, H. T. Hsu, T. J. Huang, H. J. Jhang, and H. T. Chou, “A circularly-polarized shaped-beam antenna array for radio frequency identification (RFID) reader applications at 2.4 GHz,” *2012 IEEE Int. Conf. Wirel. Inf. Technol. Syst. ICWITS 2012*, 2012, doi: 10.1109/ICWITS.2012.6417760.

[20] W. Ali *et al.*, “Design and Analysis of a Quad-Band Antenna for IoT and Wearable RFID Applications,” *Electron. 2024, Vol. 13, Page 700*, vol. 13, no. 4, p. 700, Feb. 2024, doi: 10.3390/ELECTRONICS13040700.

[21] W. Ali, Nizam-Uddin, M. Zahid, and S. Shoaib, “Performance Analysis and Design Optimization of Wearable RFID Sensor-Antenna System for Healthcare Applications,” *IEEE Access*, vol. 13, pp. 145540–145555, 2025, doi: 10.1109/ACCESS.2025.3596519.

[22] S. S. A.-B. Md. Ashraful Haque, Md Afzalur Rahman, “Machine learning-based technique for gain and resonance prediction of mid band 5G Yagi antenna,” *Sci. Rep.*, 2023, [Online]. Available: <https://www.nature.com/articles/s41598-023-39730-1>

[23] G. S. B. Sourav Ghosh, “A dual-port, single-fed, integrated microwave and mm-wave MIMO antenna system with parasitic decoupling mechanism for 5G-enabled IoT applications,” *AEU - Int. J. Electron. Commun.*, vol. 176, no. 1, p. 155122, 2024, doi: 10.1016/j.aeue.2024.155122.

[24] M. A. Rahman, S. S. Al-Bawri, M. T. Islam, M. J. Singh, and M. A. Rahman, “A Novel Compact Ultrawideband Microstrip Patch Antenna for Satellite Communications System,” *Springer Proc. Phys.*, vol. 303, pp. 243–251, 2024, doi: 10.1007/978-981-97-0142-1\_25.

[25] M. A. Rahman, S. S. Al-Bawri, M. T. Islam, M. J. Singh, D. Saha, and M. A. Haque, “A Compact Multiband Microstrip Antenna Design for 5G IOT and Satellite Communication Applications,” *Springer Proc. Phys.*, vol. 303, pp. 125–132, 2024, doi: 10.1007/978-981-97-0142-1\_13.

[26] S. S. A.-B. Md Afzalur Rahman, “Miniaturized tri-band integrated microwave and millimeter-wave MIMO antenna loaded with metamaterial for 5G IoT applications,” *Results Eng.*, vol. 24, p. 103130, 2024, doi: <https://doi.org/10.1016/j.rineng.2024.103130>.

[27] A. J. A. A.-G. Nazrin Haziq Jemaludin, “A comprehensive review on MIMO antennas for 5G smartphones: Mutual coupling techniques, comparative studies, SAR analysis, and future directions,” *Results Eng.*, vol. 23, p. 102712, 2024, [Online]. Available: <https://www.sciencedirect.com/science/article/pii/S2590123024009678>

[28] J. L. and H. L. F. Xue, Y. Zhang, “Circularly Polarized Cross-Dipole Antenna for UHF RFID Readers Applied in the Warehouse Environment,” *IEEE Access*, vol. 11, pp. 38657–38664, 2023, doi: 10.1109/ACCESS.2023.3253542.

[29] & T. B. P. Sonali A. Kale, “Hybrid Metamaterial-Based Microwave Amplifiers for Enhanced Power Efficiency and Miniaturization in IoT Devices | Journal of RF and Microwave Communication Technologies,” *Journal of RF and Microwave Communication Technologies*. Accessed: Jan. 01, 2026. [Online]. Available: <https://matjournals.net/engineering/index.php/JoRFMCT/article/view/1267>

[30] A. A. Elena García, "Overview of Reconfigurable Antenna Systems for IoT Devices," *Electronics*, vol. 13, no. 20, p. 3988, 2024, doi: <https://doi.org/10.3390/electronics13203988>.

[31] M. A. S. A. Faroq Razzaz, Saud M. Saeed, "Compact Ultra-Wideband Wilkinson Power Dividers Using Linearly Tapered Transmission Lines," *Electronics*, vol. 11, no. 19, p. 3080, 2022, doi: <https://doi.org/10.3390/electronics11193080>.

[32] J. I. L. Junho Yeo, "Gain Enhancement of Microstrip Patch Array Antennas Using Two Metallic Plates for 24 GHz Radar Applications," *Electronics*, vol. 12, no. 7, p. 1512, 2023, doi: <https://doi.org/10.3390/electronics12071512>.

[33] A. Hossain and A. V. Pham, "A Novel Gain-Enhanced Miniaturized and Lightweight Vivaldi Antenna," *IEEE Trans. Antennas Propag.*, vol. 71, no. 12, pp. 9431–9439, Dec. 2023, doi: 10.1109/TAP.2023.3310611.

[34] M. H. J. Sahar Saleh, "Compactness and performance enhancement techniques of ultra-wideband tapered slot antenna: A comprehensive review," *Alexandria Eng. J.*, vol. 74, pp. 195–229, 2023, doi: <https://doi.org/10.1016/j.aej.2023.05.020>.

[35] A. A. R. Saba Tariq, "Metasurface based antenna array with improved performance for millimeter wave applications," *AEU - Int. J. Electron. Commun.*, vol. 177, p. 155195, 2024, doi: <https://doi.org/10.1016/j.aeue.2024.155195>.

[36] Y. F. Cheng, Z. H. Gao, W. J. Chen, C. Liao, and X. Ding, "Metasurface-Covered Planar Endfire Antenna with Vertical Polarization," *IEEE Trans. Antennas Propag.*, vol. 71, no. 6, pp. 5410–5415, Jun. 2023, doi: 10.1109/TAP.2023.3255643.

[37] C. Zhou, W. Yang, Q. Xue, Y. Liu, Y. Xu, and W. Che, "Millimeter-Wave Wideband Dual-Polarized LTCC Antenna Array Based on Metasurfaces for Beam-Scanning Applications," *IEEE Trans. Antennas Propag.*, vol. 70, no. 10, pp. 9912–9917, Oct. 2022, doi: 10.1109/TAP.2022.3177448.

[38] S. Verma, L. Mahajan, R. Kumar, H. S. Saini, and N. Kumar, "A small microstrip patch antenna for future 5G applications," *2016 5th Int. Conf. Reliab. Infocom Technol. Optim. ICRITO 2016 Trends Futur. Dir.*, pp. 460–463, Dec. 2016, doi: 10.1109/ICRITO.2016.7784999.

[39] S. Muzaffar, D. Turab, M. Zahid, and Y. Amin, "Dual-Band UWB Monopole Antenna for IoT Applications," *Eng. Proc. 2023, Vol. 46, Page 29*, vol. 46, no. 1, p. 29, Sep. 2023, doi: 10.3390/ENGPDOC2023046029.

[40] C. H. Chang, T. A. Chang, M. Z. Kuo, T. M. Koo, C. I. G. Hsu, and X. Wang, "Low-Backward Radiation Circular Polarization RFID Reader Antenna Design for Sports-Event Applications," *Electron. 2025, Vol. 14, Page 3582*, vol. 14, no. 18, p. 3582, Sep. 2025, doi: 10.3390/ELECTRONICS14183582.

[41] W. Abdelrahim and Q. Feng, "Wideband Circularly Polarized Slot Antenna for Universal UHF RFID Reader," *2018 Int. Conf. Microw. Millim. Wave Technol. ICMMT 2018 - Proc.*, Dec. 2018, doi: 10.1109/ICMMT.2018.8563580.

[42] J. H. Lu and S. F. Wang, "Planar broadband circularly polarized antenna with square slot for UHF RFID reader," *IEEE Trans. Antennas Propag.*, vol. 61, no. 1, pp. 45–53, 2013, doi: 10.1109/TAP.2012.2220103.

[43] B. Xu, S. Zhang, Y. Liu, J. Hu, and S. He, "Compact broadband circularly polarised slot antenna for universal UHF RFID readers," *Electron. Lett.*, vol. 51, no. 11, pp. 808–809, May 2015, doi: 10.1049/EL.2015.0593.

[44] E. Mireles and S. K. Sharma, "A novel wideband circularly polarized antenna for worldwide UHF band RFID reader applications," *Prog. Electromagn. Res. B*, no. 42, pp. 23–44, 2012, doi: 10.2528/PIERB12051019.

[45] S. Bhaskar, M. G. Siddiqui, S. Singhal, and A. Bansal, "Miniaturized Circularly Polarized Vicsekcross-Shaped Slot Antenna for UHF-RFID Reader Handset

Applications,” *IEEE J. Radio Freq. Identif.*, vol. 6, pp. 515–523, 2022, doi: 10.1109/JRFID.2022.3195031.

[46] C. Y. D. Sim, C. W. Lin, T. A. Chen, J. R. Liou, and H. T. Chou, “An eccentric annular slotted patch with parasitic element for UHF RFID reader applications,” *2019 IEEE Int. Conf. RFID Technol. Appl. RFID-TA 2019*, pp. 37–40, Sep. 2019, doi: 10.1109/RFID-TA.2019.8892001.

[47] I. U. Din, S. Ullah, N. Mufti, R. Ullah, B. Kamal, and R. Ullah, “Metamaterial-based highly isolated MIMO antenna system for 5G smartphone application,” *Int. J. Commun. Syst.*, vol. 36, no. 3, p. e5392, Feb. 2023, doi: 10.1002/DAC.5392.

[48] M. Y. Zeain, “A New Technique of FSS-Based Novel Chair-Shaped Compact MIMO Antenna to Enhance the Gain for Sub-6GHz 5G Applications,” *IEEE Access*, vol. 12, pp. 49489–49507, 2024, doi: 10.1109/ACCESS.2024.3380013.

[49] Y. Qin, P. Wang, Y. Wang, Z. Yan, and H. Zhou, “Wideband Fabry-Perot Cavity Antenna Based on Single-Layer Partially Reflective Surface With Multiple Resonances,” *IEEE Antennas Wirel. Propag. Lett.*, vol. 23, no. 12, pp. 4688–4692, 2024, doi: 10.1109/LAWP.2024.3465931.

[50] Q. Liu and L. Zhu, “A Compact Wideband Filtering Antenna on Slots-Loaded Square Patch Radiator under Triple Resonant Modes,” *IEEE Trans. Antennas Propag.*, vol. 70, no. 10, pp. 9882–9887, Oct. 2022, doi: 10.1109/TAP.2022.3184494.

[51] Y. I. A. Hevin A. Muhammad, “A highly flexible and low-profile metasurface antenna for wearable WBAN systems,” *Optik (Stuttg.)*, vol. 313, p. 171974, 2024, doi: <https://doi.org/10.1016/j.ijleo.2024.171974>.

[52] N. K. Sonal Jatkar, “Investigation of SAR Reduction and Bending Effect Using a Flexible Antenna with EBG Structure for 2.45 GHz Wearable Applications,” *Int. J. Intell. Syst. Appl. Eng.*, vol. 12, no. 21s, pp. 1006–1014, Mar. 2024, Accessed: Jan. 01, 2026. [Online]. Available: <https://ijisae.org/index.php/IJISAE/article/view/5499>

[53] N. Sirait, F. Fathurahman, M. Alaydrus, and U. Umaisaroh, “Design of a Textile Antenna Using Metasurface Technology for Wireless Body Area Networks,” *J. Telecommun. Electron. Control Eng.*, vol. 6, no. 2, pp. 89–96, Jul. 2024, doi: 10.20895/JTECE.V6I2.1326.

[54] H. K. Nie *et al.*, “Wearable Antenna Sensor Based on EBG Structure for Cervical Curvature Monitoring,” *IEEE Sens. J.*, vol. 22, no. 1, pp. 315–323, Jan. 2022, doi: 10.1109/JSEN.2021.3130252.

[55] S. S. Yuhao Wu, “Design of Quasi-Endfire Spoof Surface Plasmon Polariton Leaky-Wave Textile Wearable Antennas,” *IEEE Access*, 2022, [Online]. Available: <https://ieeexplore.ieee.org/document/9933449>

[56] M. N. Youcef Braham Chaouche, “A Wearable Circularly Polarized Antenna Backed by AMC Reflector for WBAN Communications,” *IEEE Access*, 2022, [Online]. Available: <https://ieeexplore.ieee.org/document/9693945>

[57] Y. Dong, Z. Wang, Y. Pan, and J. H. Choi, “Characterization of shorted dipole antennas for low-cost RFID reader applications,” *IEEE Trans. Antennas Propag.*, vol. 68, no. 11, pp. 7297–7308, Nov. 2020, doi: 10.1109/TAP.2020.2998163.



Copyright © by authors and 50Sea. This work is licensed under Creative Commons Attribution 4.0 International License.